al Kimiya: Jurnal Ilmu Kimia dan Terapan,
p-ISSN: 2407-1897, e-ISSN: 2407-1927
Vol. 11, No. 1 (12-28), June 2024/Djulhijah 1445

FABRICATION OF Cu MODIFIED NANO CHITOSAN WITH BROMOCRESOL GREEN AS INTELLIGENT PACKAGING

NENY RASNYANTI M ARAS[1*], ADINDA IRWANA[1], AND AMELIANA UTAMI[1]

[1]Chemical Analysis Study Program, Akademi Komunitas Industri Manufaktur Bantaeng, Bantaeng, Indonesia

[*]Corresponding Author email: neny.aras@akom-bantaeng.ac.id

Article Information

Received: Feb 15, 2024
Revised: May 22, 2024
Accepted: Jun 06, 2024
Published: Jun 29, 2024

DOI:
10.15575/ak.v11i1.33742

Keywords:
smart packaging, nano chitosan, chitosan-PVA-TPP-Cu, antibacterial packaging.

Abstract

In recent advancements, the development of smart packaging systems for food has focused on utilizing composite materials to enhance functionality and sustainability. In this study, the composite film from chitosan and PVA was combined at various concentrations (ranging from 0.1% to 0.5%) with the addition of Cu(500mM) and 1% STPP at a 5:1 ratio. An additional indicator was included to detect fish spoilage. The synthesized chitosan material was then blended with PVA to form a composite film. The film was characterized using FTIR, which confirmed the presence of fingerprint vibrations indicating the cross-linking between TPP, chitosan, and Cu. These bonds were observed at wave numbers 1118 cm-1, 879 cm-1, and 603 cm-1. SEM analysis revealed that the film had particle sizes ranging from 865 nm to 1.49 μm. XRD analysis showed distinctive features of pure chitosan and chitosan composite. The composite film K-05 produced an amorphous structure, indicating decreased crystallinity due to the addition of STPP and Cu. The water uptake test demonstrated that an increased concentration of chitosan in the composite led to higher absorption and solubility effects. Conversely, the addition of chitosan in the film decreased water vapor permeability as determined by the water vapor permeability test. The antibacterial test conducted on all films (concentration of 0.1% to 0.5%) indicated that the films K-01 and K-02 exhibited the best zone of inhibition against Escherichia coli. This study successfully synthesized and characterized a smart packaging film composed of polyvinyl alcohol (PVA), chitosan, copper (Cu), and bromocresol green (BCG) indicator, designed to monitor food freshness through visual pH changes and inhibition of microbial growth.

INTRODUCTION

The majority of synthetic plastics used today are made of petroleum which non-biodegradable. Food packaging will eventually be discarded in nature and turn into a mountain of trash. This waste will accumulate as solid waste in settlements and will eventually become an environmental issues [1], [2].

The most recent advancements in packaging technology are currently producing intelligent, environmentally friendly packaging. This packaging is separated into active packaging and smart packaging [3]. The ability of active packaging and smart packaging to interact with food and the environment is their primary point of differentiation. Through signals that are sent when physical or chemical changes occur in packaged food ingredients, smart packaging is utilized to monitor product quality [4]. While active packaging can be used to lengthen the shelf life of foodstuffs, this packaging not only serves to wrap food but also enhances food quality due to its antibacterial qualities.

Numerous investigations on antibacterial plastics have been conducted using nanoscale metal oxides and synthetic antimicrobial agents. The use of natural antibacterials has, however, become the focus of research as a result of the green industry [5]. Natural antibacterials are favored in their applications due to their characteristics like being non-toxic, environmentally friendly, and compatible [6]. Chitosan is a common substance used in food packaging because it is simple to modify, has strong barrier qualities, and can form films. Additionally, it has been demonstrated that this polymer can prevent both gram-positive and gram-negative bacteria from growing [7] also by adding filler like ZnO and CuO nanoparticles [8], [9], [10]. Antibacterial properties also can be improved by adding binahong extract. The optimal bacterial inhibition observed in the chitosan-PVA plastic was achieved by incorporating 100% binahong extract, resulting in a 12 mm inhibition zone [11].

Modification of chitosan films can be carried out by adding plasticizers [12], [13], [14]; fillers [15], and cross-linking agents [16], [17] . To boost the polymer's mobility and flexibility, the plasticizer will aid in reducing the intermolecular pressures acting on it [18]. The cross-linking agent will make pure chitosan more resistant to air and improve its mechanical properties. The incorporation of cross linkers and plasticizers will also affect other properties of the base polymer.

Using active packaging can increase the lifespan of food because it protects from microorganisms and moisture and prevents oxidation [19], [20], [21]. The natural materials used to make these films must fulfill the standards for food packaging, which are thermally stable, antioxidant, antimicrobial, biocompatible, easy to produce, and abundant in material. Besides incorporating cross-linking agents to enhance the mechanical, hydrophobic, and antibacterial properties of chitosan plastic, active substances like plant extracts can also be added [22], [23], [24]. The presence of hydroxyl and amino groups in the chitosan framework makes it have high hydrophilicity [25], [26]. On the other hand, this affects the polymer's poor mechanical strength. Several research was conducted, including through grafting, composites, and blending, to address these limitations [27], [28], [29]. PVA is one of the suitable polymers that can be blended with chitosan. Chemical characteristics and production costs may both improve when PVA and chitosan are combined [30], [31], [32]. To increase the thermal and mechanical stability of chitosan, one of the polymers used as a blending component is polyvinyl alcohol (PVA). The properties of PVA which are flexible and have better mechanical strength than chitosan, are hydrophilic [33], non-toxic, and thermally stable [37], [38] are the main reasons why PVA was chosen to be used as a blending material [39], [40].

Numerous researchers have shown interest in the combination of synthetic and natural polymers, which will result in new material characteristics. Even though its biocompatibility is good, it is expensive to produce and has poor mechanical resistance [41]. Therefore, optimization of the ratio between the two polymers must be developed. The interaction of the two polymers is expected to be able to form good intermolecular bonds thereby increasing the mechanical resistance of the polymer. The interaction between the two polymers is very good at covering their respective deficiencies. The PVA film is thicker than the pure chitosan film because of its higher surface density. When PVA and chitosan are combined, the mechanical resistance, which had already improved, can be further improved which increased with the content of chitosan due to the broad hydration layers of the charged chitosan chains [42].

According to several recent studies on plastic film packaging, the most prevalent type of research focuses on using chitosan as a primary component of packaging film. The findings indicate that the blend of chitosan, zinc oxide, and PVA has significant potential to inhibit S. aureus colony growth. This effectiveness is attributed to the enhanced dispersion of components provided by PVA, and the improved mutual activity between the metal oxide and natural polymer facilitated by the chitosan-ZnO chelate [43]. Previous study found that chitosan combined with PVA for food packaging films showed good miscibility, thermal stability, amorphous nature, and promising mechanical characteristics for packaging applications [44], [45]. Contrary to that, some researchers found that these combinations have limitations on mechanical properties and achieving optimal water vapor barrier properties [46], [47].

Based on the previous research, it can be concluded that the highest hydrogel density and tensile strength were obtained in hydrogels with a crosslinking agent concentration of 1.5% for chitosan:PVA ratio of 1:3, although this configuration also resulted in the lowest degree of swelling. Conversely, the lowest hydrogel density and tensile strength were observed with a crosslinking agent concentration of 0.5% for chitosan:PVA ratio of 3:1 [48]. When the amount of PVA is decreased, the degree of both intra- and intermolecular hydrogen bonding is reduced due to the anionic nature of the hydroxyl group. This reduction impacts the polymer’s structural integrity and flexibility [25]. A composite film with 0.025% zeolite-Ag content exhibits a tensile strength value of 46.534 MPa by combining 40% (v/v) PVA and 60% (v/v) chitosan [49]. In addition the mechanical, thermal, morphological, and sensitivity properties of chitosan/PVA to pH with the addition of glutaraldehid as a crosslinking agent [50]. The results of his research show that water uptake and thermal resistance decrease with decreasing PVA concentration. The presence of hydroxyl groups allows PVA to bond chemically with the amine groups in chitosan.

The incorporation of smaller inorganic particles into larger polymers is desirable to combine the parameters of the two materials and improve the physicochemical properties of the

polymers. The water vapor barrier properties of biopolymer films are highly dependent on the plasticizer and moisture content [51], [52], [53]. Nanoparticles (Cu nps colloids) in solution form chitosan films and the film performance of these composites depends on their barrier properties. Cardenas found that the incorporation of colloidal Cu nanoparticles in the chitosan matrix improved the film barrier properties, decreased oxygen permeability as well as water vapor permeability, and increased protection against UV rays [54], [55].

Based on the reasons above, the development of this research direction is in the manufacture of intelligent plastics that provide an antibacterial effect while being able to provide information to consumers about product conditions through changes in the color of the plastic.

EXPERIMENT

Material

$CuSO_4$, NaOH, bromocresol green (BCG), acetic acid p.a, (merck), Sodium Tripolyphosphate (STPP), Polyvinyl Alcohol, NA medium, E.Coli.

Instrumentation

The equipment used in this study included beaker glass, analytical balance, hot plate, stirring rod, a hot plate, funnel, paper filters, cylinder glass, volumetric pipettes, spatulas, aluminum foil, petri dish, incubator, autoclave desiccator, freeze dryer, SEM, and FTIR.

Procedure

Preparation of Chitosan-Cu-TPP Composite

Chitosan as much as 0.1 -0.5 g each was dissolved in 100 mL of 2% acetic acid and then filtered to remove impurities. The chitosan solution was homogenized using a magnetic stirrer for 10 minutes and added with a ratio of nano chitosan and 1% Sodium Tripolyphosphate (STPP) with a ratio of 5:1 (v/v) then continued homogenization for 1 hour at a temperature of 50°C and a speed of 400 rpm. In the next step, a mixture of 1 M NaOH and CuSO4 (500 mM) with a ratio of 1:10 (v/v) was added to the chitosan-STPP and BCG solution as much as 1:1000 of the nano chitosan-STPP mixture, then homogenized for 1 hour (temperature 50° C and a speed of 400 rpm). Wait for the solution to cool before adjusting the pH to a range of 8 to 10 to promote the creation of nanoparticles. The pH is then neutralized once more by repeated washings using distilled water until a pH of 6 to 7. The particles are centrifuged at 10,000 rpm for 20 minutes. To create nano chitosan-Cu powder, the precipitate was dried in a freeze dryer at 3-5°C

Blending Chitosan-Cu-TPP/PVA

Preparation of a homogeneous solution of chitosan-TPP/PVA by dissolving of Chitosan-Cu-TPP composite with PVA (1:1) by stirring using a magnetic stirrer with a stirring speed of 300 rpm and heated at 80^{o}C for 30 minutes.

Characterization

FTIR of chitosan-Cu-TPP and morphology of the chitosan-Cu-TPP/PVA film

FT-IR spectra from an FT-IR spectrophotometer were used to study the chemical composition of the films and any potential interactions. SEM was used for the morphological study to examine the morphology of the film.

Water absorption

Control films and nanochitosan-Cu-BCG films were stored for 3 days under atmospheric conditions. The provided film (20 × 10 mm^2) was immersed in a closed chamber containing 20 mL of distilled water (100% RH). Films were removed from distilled water at set time intervals and weighed. An analytical balance with a precision of 0.1 mg is used for weighting. Moisture absorption is calculated by the following formula:

$$Moisture\ uptake = \frac{Wt-Wi}{Wi} x100\% \qquad (1)$$

where, wt is the weight (mg) of film at a certain time and wi is the initial weight (mg).

Solubility in water

Solubility films are defined as the percent of film that is dissolved in water after submerging in water for 24 hours. Films were placed in at desiccator containing silica for 24 hours, and the initial weight of films was weighted (Wi), then the film was submerged in 20 mL distilled water for 24 h in atmospheric conditions. Finally, the films were taken out of the distilled water and transferred to the desiccator containing calcium sulfate for 24 hours again. The dried films were weighed again, and final weight was calculated (Wf), and the solubility percent was calculated as the following:

$$SP\ (\%) = \frac{Wi - Wf}{Wf} x100\% \qquad (2)$$

where, wf is the final weight (mg) of film at a certain time and wi is the initial weight (mg).

Observation of the Characteristics of Intelligent Packaging

Testing the level of fish spoilage was carried out at 30°C for 15 hours of observation.

Antibacterial Test With Disc Method

Antibacterial test was performed using coliform bacteria E. coli. Films 1x1 cm at variation of concentrations (0.1%-0.5%) were placed into NA medium containing e coli bacteria. The petri disk was then incubated for 1 day at 37°C.

RESULT AND DISCUSSION

This study's emphasis on optimizing nanoparticle fabrication is based on Calvo et al.'s (1997) methodology. To begin, chitosan containing 0.1, 0.2, 0.3, 0.4, and 0.5 grams is dissolved in a solution of 2% acetic. It is because of chitosan's excellent solubility in acidic solutions. The concentration of 2% acetic acid was identified as the most conducive for effecting chitosan dissolution [56]. Next, TPP 1% solution was added dropwise with the ratio of chitosan to TPP solution is 5:1. TPP is the crosslinker agent. A meticulous evaluation substantiated that 1% of TPP is the optimal efficacy concentration for producing produce nano-sized particles. In the fabrication of antibacterial plastic, a mixture of $CuSO_4$ and NaOH was added to the solution and homogenized for 1 hour. In this phase, the resulting film was thoroughly washed with distilled water until reaching a neutral pH level followed by 1% of BCG as an indicator. The mixture is centrifuged after washing to obtain a homogeneous, nano-sized solution. The resulting precipitate is then put through freeze-drying processes, which results in the development of a desiccated powder.

The TPP-chitosan complex was prepared by dropping chitosan droplets into the TPP solution which is called the ionic gelation method. Chitosan is first dissolved in weak acid, allowing the amine groups to undergo protonation to produce polycations. To ensure that the polycations and polyanions of TPP could interact completely, TPP was gradually introduced to the chitosan solution. There are two different crosslinking process schemes: chemical cross-linking and physical cross-linking. Because STPP is a non-toxic crosslinking agent, chemical crosslinking in this work was feasible. The negative charge on the phosphate anion in TPP and the amine cations in chitosan interacted electrostatically to produce nanoparticles [57], [58]. Due to the complexing of differing charges between chitosan and TPP, chitosan will undergo ionic gelation. When stirred, this ionic gelation can take place at room temperature.

Chitosan is dissolved in a weak acid solution to produce chitosan cations in the ionic gelation process. After that, while stirring, the solution is introduced by slowly dripping into the TPP polyanionic solution. Chitosan goes through ionic gelation and precipitation to create spherical particles as a result of complexation between various charges. Thus, mechanical production at room temperature resulted in the spontaneous formation of nanoparticles.

Based on the findings from Reddy the presence of TPP as a crosslinking agent and CTAB as a surfactant was responsible for the synthesis of chitosan nanoparticles measuring 320.8 nm [39] . Due to the presence of water, TPP will ionize and produce OH and $P_3O_{10}^{-5}$ ions. The amine groups in chitosan will interact electrostatically with the negative charge on $P_3O_{10}^{-5}$, leading to the formation of the intermolecular networks of chitosan polymers via ionic bridges, as can be seen in **Figure 1** [58], [59].

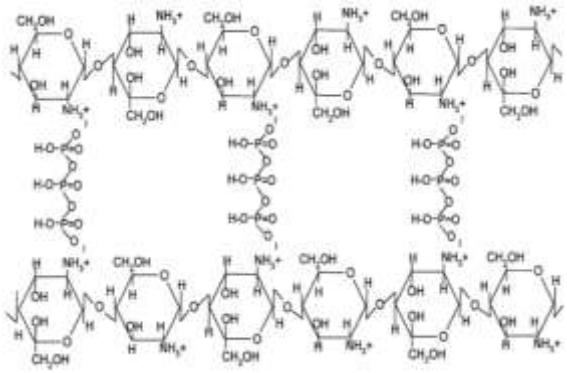

Figure 1. Cross-linking between chitosan and sodium tripolyphosphate.

Chitosan can dissolve well at a weak acid pH which then protonates to form cationic polyamines ($-NH_3^+$). TPP that undergoes dissociation produces 3 negative charges originating from phosphates so that it can be said to be a polyanion. This chitosan cation will interact very well with the TPP polyanion. It should be noted that the ratio of the addition of TPP in the solution must be appropriate [60] [61], because the excess addition will make the

particle size enlarge. Therefore, it would be very good if added with surfactants so that agglomeration can be prevented like tween-80 [62], [63]. The size and surface charge of the particles can be modified by varying the ratio of chitosan to stabilizer.

Although TPP can bind to most of the amine groups in chitosan, not all of the chitosan charges bind to it during the formation resulting in the charge density of the polymer is being positively charged which is a characteristic of chitosan nanoparticles:TPP [64], [65].

According to Vera, PVA is a polymer that is hydrophilic, non-toxic, and elastic. This characteristic enables compatibility with chitosan while blended [66]. PVA /chitosan films were produced using the solvent casting technique. Chitosan films have a lower degree of flexibility than pure PVA films [44]. The hydrophilic PVA that is added to the chitosan polymer is meant to make the film mechanically strong[66].

Membrane printing was conducted at the glass transition temperature of PVA, which is 80°C. As indicated by certain references, the linkage established between PVA and chitosan is attributed to hydrogen bonding. This interaction through hydrogen bonds contributes to enhancing the film's strength. The membrane's structure becomes more compact when PVA occupies the hydrogel cavity, resulting in what is known as an interpenetrating network (IPN). The blending of PVA and chitosan involves both the physical arrangement of polymer chains and chemical bond formation, leading to heightened mechanical properties of the polymer. This interaction imparts increased strength and linearly escalates the polymer's thickness with the addition of PVA.

The blending of chitosan and PVA is initiated once the chitosan solution reaches homogeneity. The incorporation of PVA solution is typically at a concentration of approximately 3%. The blending process of chitosan and PVA at specific proportions enhances the film's architecture, rendering it denser [67]. This structural enhancement contributes to fortifying the membrane's strength and its ability to stabilize the resulting membrane structure [68]. Moreover, the introduction of PVA leads to an increase in the film's thickness [69].

FTIR

FT-IR spectroscopic analysis was conducted to explore the molecular-level interaction within chitosan/TPP/Cu films. The FT-IR spectrum was acquired for both pure chitosan powder and the chitosan/TPP/Cu composite. In the case of pure chitosan, as reported by Kumar, the absorption peak at 1250 cm^{-1} signifies the presence of amino groups. The principal saccharide-related groups are represented by bands at 890, 1020, and 1150 cm^{-1}, while the strain in amino groups is indicated by the 3340 cm^{-1} band (OH), and the amide I and amide II bands are seen at 1660 cm^{-1} and 1560 cm^{-1}, respectively

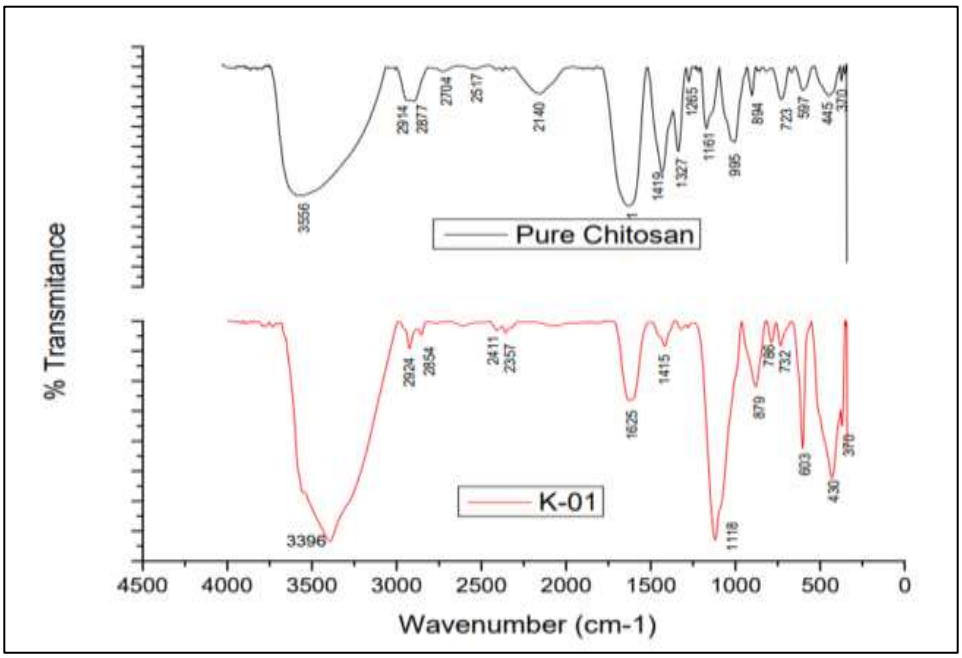

Figure 2. FTIR spectra on chitosan and K-01 (0.1% chitosan/TPP/Cu).

Based on the results of this study, the broad absorption band shown at 3300 to 3500 cm−1 corresponds to the O—H stretching for all spectra. In the case of pure chitosan powder, the absorption peak observed at 3556 cm^{-1} corresponds to the combined strain of NH_2 and OH groups.

Table 1. Characteristics absorption bands (cm^{-1}) in infrared spectra

Functional Group	Chitosan (cm^{-1})	Chitosan/Cu/TPP (k-01) (cm^{-1}) powder	Chitosan
-OH and –NH2 axial stretch	3556	3396	3377 3302 [70] [71]
-C-H- axial stretch	2924-2854	2914-2877	2911 [72]
Copling C-N axial stretch	1327	1321	1324 [72]
Copling C-O axial stretch	1419	1415	1406 [72]
Amino group	1265		1250 [72]
N-H angular deformation	1611	1625	1660 dan 1560 (amida I dan II) [72]
Hydroxyl group (OH) in polymer and secondary amine (NH)	1161	1118	
Strain (Cu-N)		430	442 [73]
Amide strain with Cu	-	603	-
P-O (stretch)	-	879	-
Saccharide	894, 1161	-	890,1150,1020[1] [71]

However, when chitosan is doped with STPP-$CuSO_4$, the broader and prominent mainly shifted to a lower wavenumber at 3396 cm^{-1}. This shift signifies a robust interaction between these groups and $CuSO_4$ and STPP. The absorption bands at 2925, 2914, 2877, and 2882 cm^{-1} are linked to the asymmetric stretching of CH_3 and CH_2 in the chitosan polymer. Additionally, the absorption peaks detected at 1611 and 1625 cm^{-1} are likely related to the bending vibrations of the $–NH_2$ groups.

In comparison to the chitosan spectrum, new absorption peaks emerge at 879 cm^{-1} and 603 cm^{-1}, attributed to the presence of the amide group and the strain mode of Cu, respectively. Another intriguing observation is the shift of the characteristic peak in **Figure 2** to a lower wavenumber. Specifically, the peak width at 3556 cm^{-1}, corresponding to the stretching vibration of hydroxyl, amino, and amide groups, undergoes a significant shift to 3396 cm^{-1}. This shift is not only accompanied by increased breadth but also heightened intensity, indicating a potent interaction between these groups and Cu and STPP.

There is some change in the absorption band after the addition of TPP and Cu. The presence of phosphate compounds is signaled by absorption at wavenumbers 786 and 732 cm^{-1}, indicative of PO stretching. On the other hand, some peaks that were present in the TPP/Cu composite chitosan are absent, specifically those at 955, 850, and 810 cm^{-1}. These changes are postulated to stem from the cross-linking interaction between the ionic charge of TPP and the positively charged amino acid segment of chitosan ($R\text{-}NH_3^+$). The cross-linking reaction between the amino group and tripolyphosphate (TPP) is supported by the reaction mechanism shown in **Figure 3**.

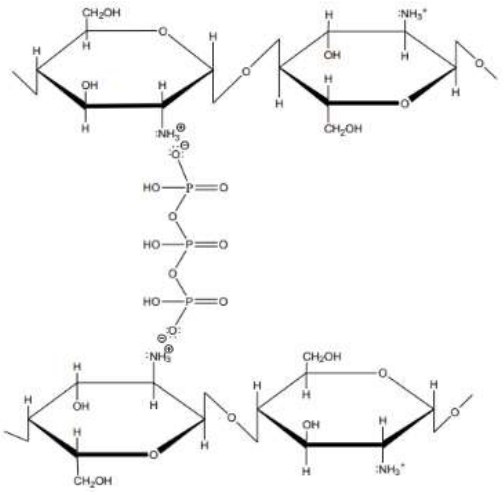

Figure 3. Cross-linking ionic chitosan and tripolyphosphate [74].

XRD Test

The X-ray diffraction (XRD) analyses of both chitosan and chitosan-tripolyphosphate at various concentrations of chitosan (0.1-0.5%) are depicted in **Figure 4**. In the X-ray diffraction patterns of the initial chitosan samples, a characteristic peak appeared at 2θ of 19.97°, indicating the presence of a linear crystalline structure within the sample. In the case of the

chitosan-TPP diffraction pattern, the peak at 2θ of 12.96° shifted to 20.42° for chitosan-TPP with chitosan concentrations ranging from 0.1 to 0.5. This peak shift across the five chitosan/TPP/Cu samples suggests a modification in the crystal structure. Consequently, it becomes evident that a transition from a crystalline structure to an amorphous one occurred in chitosan due to the formation of cross-links between TPP and chitosan.

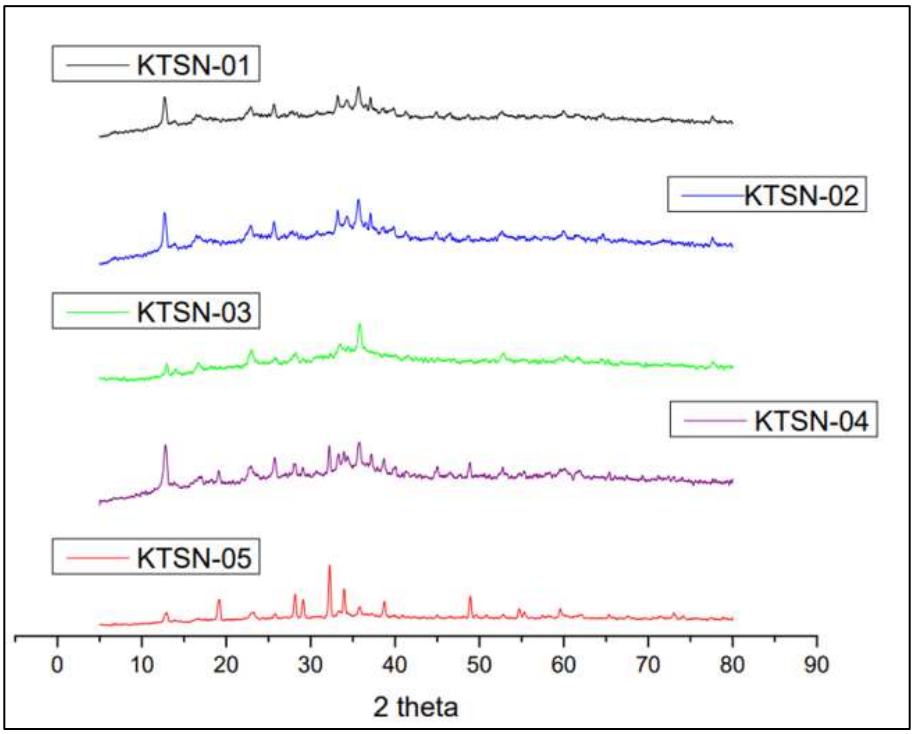

Figure 4. Illustration of the X-ray diffraction patterns in chitosan/TPP/Cu ; a) 0.1%, b) 0.2% , c) 0.3%, d) 0.4%, and, e) 0.5% .

SEM

Figure 5 depicts the morphology of the chitosan/Cu/TPP composite powder. The observed particle sizes range from 865 nm to 1.49 μm. In general, the resulting chitosan/Cu/TPP powder composites exhibit a micrometer scale rather than a nano size. The surface structure obtained resembles that of a tube, similar to findings in previous research [75]. The SEM results reveal that the quantity of chitosan used for composite formation influences the particle size. Greater amounts of chitosan lead to larger particle sizes in the produced chitosan/Cu/BCG composite powder due to agglomeration. Notably, a comparison between chitosan K-0.1 and K-0.5 films shows distinct differences; K-0.1 displays lump-like structures, unlike K-0.5.

The incorporation of chitosan into the TPP/Cu composite contributes to an increased surface area of the composite. This is evident in the films where, upon blending with PVA, an inhomogeneous structure emerges. As seen in **Figure 6**, the shape of the composite film surface in K-05 is tubular, while in K-01 it is granular. This means that the ratio of chitosan addition in the composite affects the shape of the film surface. Additionally, the appearance of films from K-0.3 to K-0.5 tends to be green due to BCG addition, signifying an acidic tendency. This color shift is attributed to heightened protonation in chitosan. The combination of chitosan composite and PVA restricts the free volume of the matrix due to chitosan addition.

Figure 5. Composite when dissolved in distilled water (from left to right K-0.1 to K.05).

However, the film's stiffness is predominantly determined by its hygroscopic characteristics. Notably, K-0.1 chitosan/PVA films exhibit greater stiffness due to the smaller composite particle size, which compresses the film's microstructure. The surface displays roughness and a prevalent crystal structure, indicating a highly polycrystalline nature.

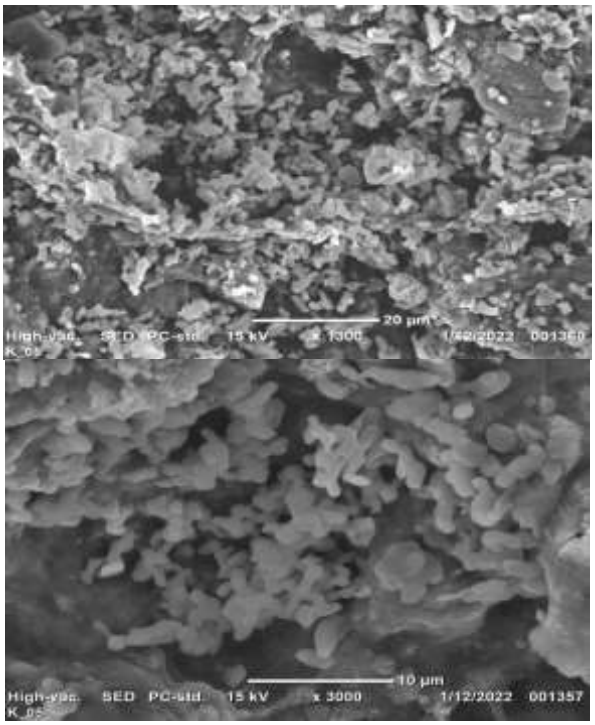

(a)

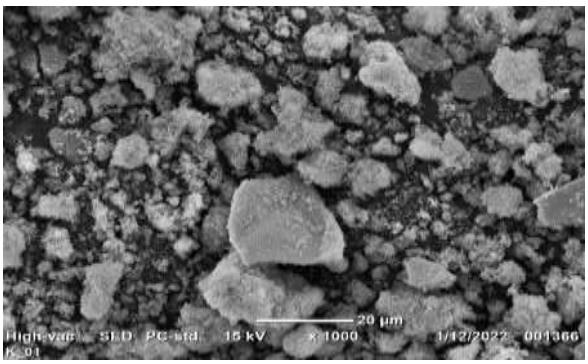

(b)

Figure 6. Structure of powder chitosan/Cu/TPP (a)K-05 (b)K-01 at 1300x and 3000x magnification.

Absorptivity and Solubility Test

Regarding the utilization of the chitosan/TPP/Cu/PVA. nano chitosan composite film as a smart indicator, the film's physical attributes necessitate testing. Fig. 7 offers insights into various chitosan variations (from K-01 to K-05) concerning their water solubility and absorption characteristics.

The findings reveal that the incorporation of chitosan, which exhibits a notable affinity for water molecules in the chitosan/TPP/Cu/PVA film, impacts the film's water absorption and solubility. Water vapor transmission is influenced by diffusivity and solubility in water. Notably, among the five chitosan film variations, (K-05) shows the highest solubility and water absorption. The higher chitosan content in this film prompts a lack of compactness among film constituents. During the blending process with PVA, chitosan tends to solvate with water molecules in PVA solution, leading to the substantial particle size of K-05. To prevent water diffusion, chitosan with a smaller particle size is desirable because this chitosan/Cu/TPP powder will fill the lattice on the PVA film when blended. Achieving a more uniform and denser blending between molecules curtails the diffusion of water vapor across the film. The influence of chitosan/TPP/Cu/PVA composite powder variations on humidity and water solubility is shown in **Figure 7** below which shows this water uptake is quite similar to the research of [76].

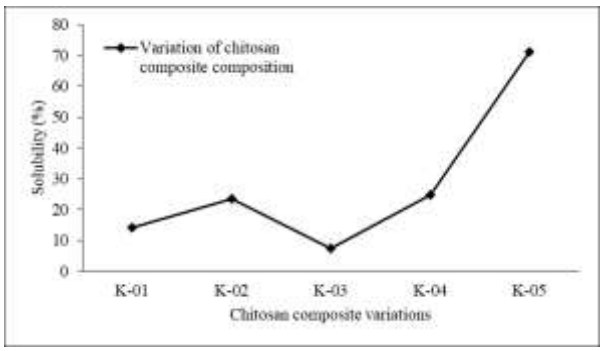

(a)

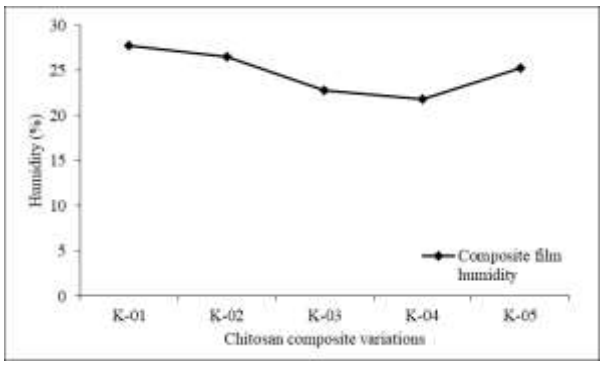

(b)

Figure 7. Effect of chitosan composition on chitosan/TPP/Cu/PVA film on (a) water solubility and (b) moisture absorption.

The water and moisture uptake showed in **Figure 7** are alighn with the previous result from Priyadharsih as presented in **Tabel 2**.

Tabel 2. Physicochemical Properties of film CS/CS/CSG.

Film Type	Physicochemical Properties			
	Moisture Content (%)	Water Absorption (%)	Solubility (%)	Opacity (A_{600} /mm)
CS	22.14 ±0.99	495.24±11.34	23.91±1.38	1.716±0.002
CSCG	15.70±0.97	63.20±2.48	34.42±1.49	0.320±0.002

Source : [76]

Biodegradable films tend to dissolve in water, which is a pivotal property of intelligent food packaging. Increasing chitosan concentration from 0.1% to 0.5% in the packaging process leads to a bigger particle size of the chitosan/Cu/TPP composite powder. The amount of chitosan concentration significantly influences its water absorption. This increase engenders a more fragile intra-polymer/film network. Simultaneously, the hydrophilic side of chitosan's active group easily combines with water molecules which impact on disrupting the hydrogen bond and also diminishing the cohesiveness of the chitosan matrix.

In terms of packaging durability, the insolubility of the film in water is desirable, but some film applications want the opposite characteristic, like in food encapsulation applications. Chitosan's hydrophilicity properties impact permeability, thickness, and stability. Aligning to Miya as noted in Ayuni, the hydrophilic attributes of PVA film rise with chitosan addition. The amalgamation of PVA and chitosan enhances the film's mechanical properties through the formation of hydrogen bonds between the two components [77], [78].

The decline in water vapor permeability of the chitosan/Cu/TPP/PVA film, coupled with varied chitosan concentrations, may be influenced by three factors: (1) hydrogen bonding interaction between chitosan and solvation, limiting chitosan hydroxyl group availability for water bonding; (2) heightened roughness contributing to diffusion path tortuosity, consequently affecting permeability. The presence of 0.1% Cu content in the chitosan/Cu/TPP/PVA film elevates the chitosan film's thickness, thus contributing to the second factor.

The increased degree of swelling due to the addition of chitosan could be due to the density of the PVA molecules that fill the hydrogel cavities. The addition of chitosan will increase the number of crosslinks in the film so that water will find it difficult to diffuse in the hydrogel. The swelling mechanism becomes more effective in an acidic environment in comparison to an alkaline one [79]. This is because it will trigger protonation of the amine groups of chitosan. Protonation will cause an increase in electrostatic repulsion. Subsequently, hydrogen bonds within the film fracture, rendering the hydrogel structure more porous and facilitating diffusion.

The hydrophilic equilibrium of the system causes the hydrogel film to move into the polymer network, resulting in changes in the dimensions of the swollen film. Figure 7 illustrates the swelling behavior of films with various chitosan content ranging from 0.1% to 0.5%. The results indicate that the increase of chitosan aligns with the water uptake. This phenomenon leads to the crosslinking between STPP as a cross-linking agent also the contribution of the blending PVA/chitosan. Based on the quantity of chitosan that is contained in the film, hydrophilic film is increasing and is associated with higher air permeability temperatures. An increase in crosslinkers leads to a decrease in swelling degree. The intra-polymer chain reactions stiffen the network, reducing flexibility and limiting the rate of swelling of hydrophilic hydrogel groups. This finding aligns with the hydrogel mechanism.

Chemical cross-linking between PVA or chitosan chains occurs at the microstructure scale. Although this study differs from others on chitosan, similar trends in the swelling behavior of PVA and chitosan support the findings. PVA can swell up to 400%, while chitosan can swell by about 200%, influenced by factors such as the solution medium, pH, and temperature [3].

Antibacterial Test

This study uses E. coli bacteria as a representation of bacteria that contaminate food. The antibacterial test was carried out by dissolving the chitosan composite nanoparticles in various concentrations of chitosan (0.1, 0.2, 0.3, 0.4, and 0.5) with 5% PVA in distilled water with a ratio of 1:2. Chitosan composite powder was tested in several pH ranges from 1 to 9, and the color appears as shown in **Figure 8**.

Figure 8. Color change of chitosan/TPP/Cu/BCG powder composite at various pH (a) 1-4 (b) 5-9.

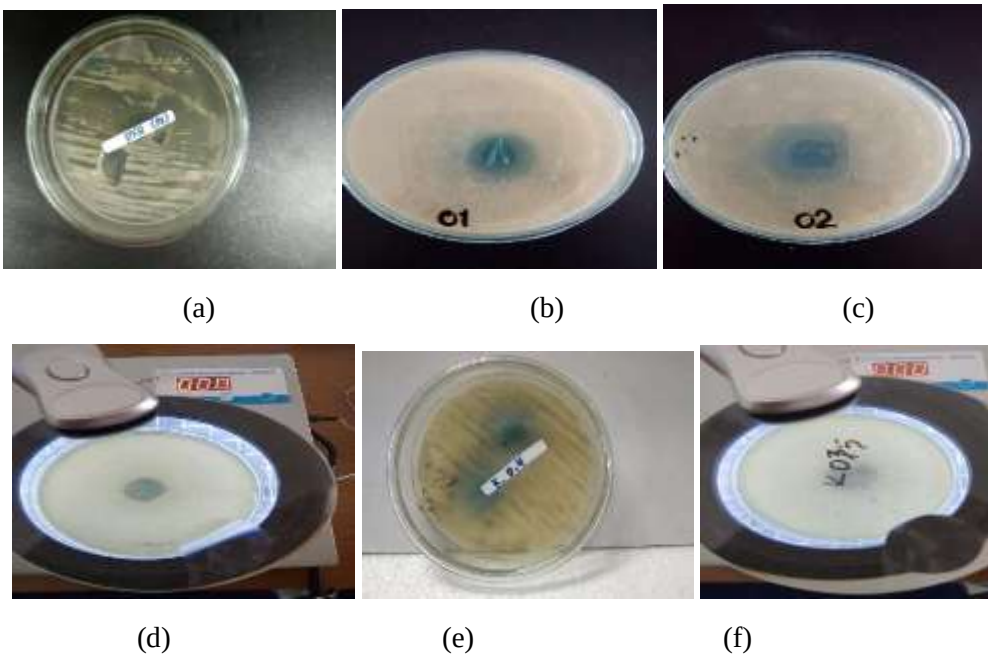

(a) (b) (c)

(d) (e) (f)

Figure 9. Antibacterial inhibition zone of PVA-chitosan/TPP/Cu/BCG composite film with e coli bacteria (a) Pure PVA (b) K01 (c) K-02 (d) K-03 (e) K-04 (f) K-05.

To see the antibacterial activity of the resulting composite film, the inhibition can be seen in **Figure 9**. It shows the diameter of the clear zone in E. coli after administration of chitosan/Cu/BCG chitosan composite nanoparticles on NA medium. The antibacterial activity of the produced chitosan composite films can be observed in Figure 8. The image shows the clear zone diameter of E. coli after the application of chitosan/TPP/PVA film on NA medium. The results indicate that the higher the concentration of chitosan in chitosan/TPP/PVA film, the smaller the clear zone where E. coli does not grow. This is because chitosan is an organic compound that can be digested by bacteria. The antibacterial ability of the nanoparticles at different chitosan concentrations varies because the particle size increases with higher chitosan concentration, resulting in higher water solubility and increased aggregation, leading to lower antibacterial activity.

Numerous previous researchers have attributed the antimicrobial properties of chitosan (Ch) to the positively charged amino groups, which interact with negatively charged proteins in microbial cells, leading to the leakage of intracellular constituents [80], [81], [82], [83], [84]. Additionally, PVA itself does not inherently possess antibacterial properties solely due to its resistance to oxygen. Instead, PVA's antibacterial activity is often enhanced through modifications or by combining it with other substances [85]. Supported this explanation some researchers found a decrease in the number of aerobic bacteria in the control sample [86], [87].

According to Coma as cited in R.Goy (2009), chitosan's antimicrobial activity involves three different mechanisms. Firstly, there is an interaction between the positive charge of chitosan molecules and the negative charge on the microbial cell membrane. This electrostatic interaction between the protonated NH_3^+ groups and the negative residues competes with Ca^{2+} on the electronegative side of the cell membrane, leading to changes in membrane permeability and triggering an internal osmotic pressure imbalance that inhibits microbial growth. Additionally, the electrostatic interaction causes peptidoglycan hydrolysis in the microbial cell wall, resulting in the release of intracellular electrolytes such as potassium ions, proteins, and nucleic acids. Secondly, chitosan in nanoparticle form can penetrate bacterial cell walls, bind to DNA, and inhibit mRNA synthesis and DNA transcription [88].

The third mechanism involves the chelation of metals, which can suppress spore elements and bind essential nutrients for microbial growth. Chitosan's ability to bind metals is due to the presence of amino groups in chitosan, which can chelate metal cations. This leads to chitosan molecules surrounding the metal complexes in bacteria, blocking some nutrient flow, and ultimately causing microbial cell death [89], [90].

Similar studies from Liu, the films exhibited significant antimicrobial activity, with higher inhibition zones observed for films containing Cu

compared to the control film. This antimicrobial effect can be attributed also because it releases Cu^{2+} ions from the nanoparticles, which have antimicrobial properties [46].

The visual appearance of the intelligent packaging sensor comprising chitosan/TPP/Cu/PVA with BCG as an indicator, along with the color alteration pattern of the sensor during the 15-hour observation of fish decay, reveals a transformation in the smart packaging color from blue to brown as seen in **Figure 10**. The working principle of smart packaging with additional BCG as an indicator on fishery products as an acid-base indicator changes color due to changes in pH. For fishery products, during fish spoils, microbial activity leads to the breakdown of proteins then produces volatile amine compounds such as trimethylamine (TMA), ammonia (NH_3), and dimethylamine (DMA). These volatile basic components interact with the indicators on the packaging and change the color of the indicator to brown. Simply, fresh fish sign with the acidic condition (the plastics are still blue) when the environment turns to a basic environment due to the presence of volatile amine the color will change. These findings align with prior research employing the Bromocresol Green (BCG) sensor [91], [92]. In their study, cellulose-acetate-based packaging films exhibited an absorbance shift from 438 nm (acidic form) to 615 nm (alkaline form) when placed in an alkaline environment.

Figure 10. Illustrates the visualization of color change in the smart packaging sensor with Chitosan/Cu/ PVA as the base material and the BCG indicator.

The underlying mechanism is believed to stem from the interaction between the carboxyl and amine groups within chitosan and the volatile bases generated during fish decay. Each volatile base adheres to the surface functional groups on the film, leading to the color change in the BCG sensor [93]. Specifically, the negatively charged chitosan interacts with volatile bases, while the positively charged amine binds to the negatively charged OH group in BCG. The accumulation of volatile base compounds binding to chitosan triggers deprotonation (transition to an alkaline state) in BCG, resulting in the color shift of the film from blue to brown.

CONCLUSION

The synthesis of chitosan composites has been successfully carried out by mixing TPP, Cu, and BCG as candidates for smart sensors and anti-bacterial packaging. The FTIR analysis further confirms the existence of numerous functional groups such as amides, amine bonds, and cross-links with TPP in addition to Cu-chitosan composites. Their utility in sensor applications largely stems from the reactivity of these functional groups towards specific analytes. The amides and amines content in the composite can better sense environmental perturbation like pH or certain ions presence making it capable of working as an efficient smart sensor and also align as anti microbial activity leading to inhibits microbial growth. BCG, occurring a pH sensitive dye leads to discernible color change in response of variation in read out which adds on sensor ability. This result will be ideal for sensing and long-term monitoring of food freshness. Based on the XRD test K-05 has an amorphous structure while the addition of TPP and Cu composites decreases the crystallinity. Decreasing crystallinity are crucial packaging activity. The most recommended film composites for optimization are K-01 and K-02 because in this composition the e-coli bacteria have the widest clean zone that is not overgrown with bacteria.

ACKNOWLEDGEMENT

Thanks to the Chemical Analysis Department, Akademi Komunitas Industri Manufaktur Bantaeng. Thanks to all those who have helped when this research was carried out.

REFERENCES

[1] T. De Pilli, A. Baiano, G. Lopriore, C. Russo, and G. M. Cappelletti, “An overview on the environmental impact of food packaging”, in *Sustainable Innovations in Food Packaging*, T. De Pilli, A. Baiano, G. Lopriore, C. Russo, and G. M. Cappelletti, Eds., Cham: Springer International Publishing, 1-14, 2021, https://doi.org/10.1007/978-3-030-80936-2_1

[2] R. Dani, K. Tiwari, and A. P. B. Prabhakar, “A review of food packaging materials and its impact on environment”, *AIP Conference*

Proceedings, **2978**(1), 020006, 2024, https://doi.org/10.1063/5.0182889

[3] G. Fuertes, I. Soto, R. Carrasco, M. Vargas, J. Sabattin, and C. Lagos, "Intelligent packaging systems: sensors and nanosensors to monitor food quality and safety", *Journal of Sensors*, **2016**(4046061), 2016, https://doi.org/10.1155/2016/4046061

[4] K. B. Biji, C. N. Ravishankar, C. O. Mohan, and T. K. Srinivasa Gopal, "Smart packaging systems for food applications: a review", *Journal of Food Science Technology*, 52(10), 6125–6135, 2015, https://doi.org/10.1007/s13197-015-1766-7

[5] C. G. Otoni, P. J. P. Espitia, R. J. Avena-Bustillos, and T. H. McHugh, "Trends in antimicrobial food packaging systems: Emitting sachets and absorbent pads", *Food Research International*, **83**, 60–73, 2016, https://doi.org/10.1016/j.foodres.2016.02.018

[6] P. J. P. Espitia, W.-X. Du, R. D. J. Avena-Bustillos, N. D. F. F. Soares, and T. H. McHugh, "Edible films from pectin: Physical-mechanical and antimicrobial properties - A review", *Food Hydrocolloids*, **35**, 287–296, 2014, https://doi.org/10.1016/j.foodhyd.2013.06.005

[7] M. Hosseinnejad and S. M. Jafari, "Evaluation of different factors affecting antimicrobial properties of chitosan", *International Journal of Biological Macromolecules*, **85**, 467–475, 2016, https://doi.org/10.1016/j.ijbiomac.2016.01.022

[8] R. Dadi, R. Azouani, M. Traore, C. Mielcarek, and A. Kanaev, "Antibacterial activity of ZnO and CuO nanoparticles against gram positive and gram negative strains", *Materials Science and Engineering: C*, **104**, 109968, 2019, https://doi.org/10.1016/j.msec.2019.109968

[9] F. Hemmati *et al.*, "The assessment of antibiofilm activity of chitosan-zinc oxide-gentamicin nanocomposite on *Pseudomonas aeruginosa* and *Staphylococcus aureus*", *International Journal of Biological Macromolecules*, **163**, 2248–2258, Nov. 2020, https://doi.org/10.1016/j.ijbiomac.2020.09.037

[10] M. Salas-Orozco, N. Niño-Martínez, G.-A. Martínez-Castañón, F. T. Méndez, M. E. C. Jasso, and F. Ruiz, "Mechanisms of resistance to silver nanoparticles in endodontic bacteria: a literature review", *Journal of Nanomaterials*, **2019**, 1–11, 2019, https://doi.org/10.1155/2019/7630316

[11] N. R. M. Aras, M. F. Lestari, and A. Irwana, "Synthesis of Smart Packaging Based on Chitosan-PVA/Binahong Extract as an Antibacterial Plastic", *ICA*, 13–22, 2024, https://doi.org/10.20956/ica.v17i1.31419

[12] X. Zhang, Z. Zhang, W. Wu, J. Yang, and Q. Yang, "Preparation and characterization of chitosan/Nano-ZnO composite film with antimicrobial activity", *Bioprocess Biosystem Enggineering*, **44**(6), 1193–1199, 2021, https://doi.org/10.1007/s00449-021-02521-x

[13] M. Aslam and M. M. A. Kalyar, "Fabrication of nano-CuO-loaded PVA composite films with enhanced optomechanical properties," *Polymer Bulletin*, **78**, 2021, https://doi.org/10.1007/s00289-020-03173-9

[14] R. N. Annisa, R. A. Lusiana, G. Gunawan, and H. Muhtar, "Optimization of chitosan-carboxymethyl chitosan membrane modification with PVA to increase creatinine and urea permeation efficiency", *Jurnal Kimia Sains dan Aplikasi.*, **27**(4), 189–196, Apr. 2024, https://doi.org/10.14710/jksa.27.4.189-196

[15] M. Aslam, Z. A. Raza, and A. Siddique, "Fabrication and chemo-physical characterization of CuO/chitosan nanocomposite-mediated tricomponent PVA films", *Polymer Bulletin*, **78**(4), 1955–1965, 2021, https://doi.org/10.1007/s00289-020-03194-4

[16] R. Eivazzadeh-Keihan *et al.*, "Review: the latest advances in biomedical applications of chitosan hydrogel as a powerful natural structure with eye-catching biological properties", *Journal of Material Science*, **57**(6), 3855–3891, 2022, dhttps://doi.org/10.1007/s10853-021-06757-6

[17] B. Zhu *et al.*, "A pH-neutral bioactive glass empowered gelatin–chitosan–sodium phytate composite scaffold for skull defect repair", *Journal of Materials Chemistry B*, **11**(40), 9742–9756, 2023, https://doi.org/10.1039/D3TB01603J

[18] M. G. A. Vieira, M. A. da Silva, L. O. dos Santos, and M. M. Beppu, "Natural-based plasticizers and biopolymer films: A review", *European Polymer Journal*, **47**(3),254–263, 2011, https://doi.org/10.1016/j.eurpolymj.2010.12.011

[19] R. K. Deshmukh, L. Hakim, and K. K. Gaikwad, "Active Packaging Materials", *Current Food Science Technology Reports*, **1**(2), 123–132, 2023, https://doi.org/10.1007/s43555-023-00004-6

[20] A. Siddiqui and K. Chand, "Enhancement of shelf life of food using active packaging technologies", *Springer International Publishing*, 133–143, 2022 https://doi.org/10.1007/978-3-030-90549-1_8

[21] H. Ahari and S. P. Soufiani, "Smart and Active Food Packaging: Insights in Novel Food Packaging", *Frontiers Microbiology.*, **12**, 2021, https://doi.org/10.3389/fmicb.2021.657233

[22] V. A. Pereira, I. N. Q. De Arruda, and R. Stefani, "Active chitosan/PVA films with anthocyanins from Brassica oleraceae (Red Cabbage) as Time–Temperature Indicators for application in intelligent food packaging", *Food Hydrocolloids*, **43**, 180–188, 2015, https://doi.org/10.1016/j.foodhyd.2014.05.014

[23] D. K. Chandra, A. Kumar, and C. Mahapatra, "Fabricating Chitosan Reinforced Biodegradable Bioplastics from Plant Extract with Nature Inspired Topology", *Waste Biomass Valorization*, **15** (4), 2499–2512, 2024, https://doi.org/10.1007/s12649-023-02293-3

[24] P. Cazón and M. Vázquez, "Mechanical and barrier properties of chitosan combined with other components as food packaging film", *Environment Chemistry Letters*, **18**(2), 257–267, 2020, https://doi.org/10.1007/s10311-019-00936-3

[25] A. Abraham, P. A. Soloman, and V. O. Rejini, "Preparation of Chitosan-Polyvinyl Alcohol Blends and Studies on Thermal and Mechanical Properties", *Procedia Technology*, **24**, 741–748, 2016, https://doi.org/10.1016/j.protcy.2016.05.206

[26] P. Ramasamy and A. Shanmugam, "Characterization and wound healing property of collagen-chitosan film from Sepia kobiensis (Hoyle, 1885)", *International Journal of Biological Macromoleculs*, **74**, 93–102, 2015, https://doi.org/10.1016/j.ijbiomac.2014.11.034.

[27] T. Ayode Otitoju, A. Latif Ahmad, and B. Seng Ooi, "Recent advances in hydrophilic modification and performance of polyethersulfone (PES) membrane via additive blending", *RSC Advances*, **8**(40), 22710–22728, 2018, https://doi.org/10.1039/C8RA03296C

[28] A. R. Pandey, U. S. Singh, M. Momin, and C. Bhavsar, "Chitosan: Application in tissue engineering and skin grafting", *Journal of Polymer Research*, **24**(8), 125, 2017, https://doi.org/10.1007/s10965-017-1286-4

[29] J. Fourie, F. Taute, L. du Preez, and D. de Beer, "Chitosan Composite Biomaterials for Bone Tissue Engineering—a Review", *Regenerative Engineering Translational Meicine.*, **8**(1), 1–21, 2022, https://doi.org/10.1007/s40883-020-00187-7

[30] V. O. Kudyshkin *et al.*, "Features of Synthesis of Graft Copolymers of Chitosan and Acrylic Acid", *Polymer Science Series B*, May 2024, https://doi.org/10.1134/S1560090424600165

[31] Z. Czibulya *et al.*, "The Effect of the PVA/Chitosan/Citric Acid Ratio on the Hydrophilicity of Electrospun Nanofiber Meshes", *Polymers*, **13**(20), 2021, https://doi.org/10.3390/polym13203557

[32] J. M. Dodda *et al.*, "Biocompatible hydrogels based on chitosan, cellulose/starch, PVA and PEDOT:PSS with high flexibility and high mechanical strength", *Cellulose*, **29**(12), 6697–6717, Aug. 2022, https://doi.org/10.1007/s10570-022-04686-4

[33] E. Y. Wardhono *et al.*, "Modification of Physio-Mechanical Properties of Chitosan-Based Films via Physical Treatment Approach", *Polymers*, **14** (23), 2022, https://doi.org/10.3390/polym14235216

[34] J. Jegal and K.-H. Lee, "Chitosan membranes crosslinked with sulfosuccinic acid for the pervaporation separation of water/alcohol mixtures", *Journal of Applied Polymer Science*, **71**(4), 671–675, 1999, https://doi.org/10.1002/(SICI)1097-4628(19990124)71:4<671::AID-APP19>3.0.CO;2-T

[35] S. K. Mallapragada and N. A. Peppas, "Dissolution mechanism of semicrystalline poly(vinyl alcohol) in water", *Journal of Polymer Sciences B Polymer. Physic*, **34**(7), 1339–1346, 1996, doi: https://doi.org/10.1002/(SICI)1099-0488(199605)34:7<1339::AID-POLB15>3.0.CO;2-B

[36] L. Rahman and J. Goswami, "Poly(Vinyl Alcohol) as Sustainable and Eco-Friendly Packaging: A Review", *Journal of Package Technology Research*, **7**(1), 1–10, 2023, https://doi.org/10.1007/s41783-022-00146-3

[37] Z. A. Alhulaybi and I. Dubdub, "Kinetics Study of PVA Polymer by Model-Free and Model-Fitting Methods Using TGA", *Polymers*, **16**(5), 2024, https://doi.org/10.3390/polym16050629

[38] A. A. Rowe, M. Tajvidi, and D. J. Gardner, "Thermal stability of cellulose nanomaterials and their composites with polyvinyl alcohol (PVA)", *Journal of Thermal Analysi and Calorimetry*, **126**(3), 1371–1386, Dec. 2016, https://doi.org/10.1007/s10973-016-5791-1

[39] E. Marin, J. Rojas, and Y. Ciro, "A review of polyvinyl alcohol derivatives: Promising materials for pharmaceutical and biomedical applications", *African Journal of Pharmacy and Pharmacology*, 2014, Accessed: Aug. 10, 2023. [Online]. Available: https://www.semanticscholar.org/paper/A-review-of-polyvinyl-alcohol-derivatives%3A-for-and-Marin-Rojas/a2eb0a887133b578aaea0db03a42fbad1df95359

[40] U. K. Parida, A. K. Nayak, B. K. Binhani, and P. L. Nayak, "Synthesis and Characterization of Chitosan-Polyvinyl Alcohol Blended with Cloisite 30B for Controlled Release of the Anticancer Drug Curcumin", *Journal of Biomaterials and Nanobiotechnology*, **02**(04), 414–425, 2011, https://doi.org/10.4236/jbnb.2011.24051

[41] M. S. B. Reddy, D. Ponnamma, R. Choudhary, and K. K. Sadasivuni, "A Comparative Review of Natural and Synthetic Biopolymer Composite Scaffolds", *Polymers*, **13**(7), 2021, https://doi.org/10.3390/polym13071105

[42] J. Bonilla, E. Fortunati, L. Atarés, A. Chiralt, and J. M. Kenny, "Physical, structural and antimicrobial properties of poly vinyl alcohol–chitosan biodegradable films", *Food Hydrocolloids*, **35**, 463–470, Mar. 2014, https://doi.org/10.1016/j.foodhyd.2013.07.002

[43] E. Cavalcante, F. Junior, M. Pereira, P. Pereira, M. Costa, and H. Oliveira, "Antibacterial activity of chitosan and zinc oxide impregnated in PVA-based membranes", *Research, Society and Development*, **12**, e23812340720, 2023, https://doi.org/10.33448/rsd-v12i3.40720

[44] W. Zhang *et al.*, "Advances in sustainable food packaging applications of chitosan/polyvinyl alcohol blend films", *Food Chemistry*, **443**, 138506, 2024, https://doi.org/10.1016/j.foodchem.2024.138506

[45] F. Liu *et al.*, "Improved hydrophobicity, antibacterial and mechanical properties of polyvinyl alcohol/quaternary chitosan composite films for antibacterial packaging", *Carbohydrat Polymer*, **312**, 120755, 2023, https://doi.org/10.1016/j.carbpol.2023.120755

[46] L. Yang *et al.*, "Preparation and characterization of PVA/arginine chitosan/ZnO NPs composite films", *International Journal of Biological Macromolecules*, **226**, 184–193, 2023, https://doi.org/10.1016/j.ijbiomac.2022.12.020

[47] J. N. N. Bueno, E. Corradini, P. R. De Souza, V. D. S. Marques, E. Radovanovic, and E. C. Muniz, "Films based on mixtures of zein, chitosan, and PVA: Development with perspectives for food packaging application", *Polymer Testing*, **101**, 107279, 2021,https://doi.org/10.1016/j.polymertesting.2021.107279

[48] B. Piluharto, A. Sjaifullah, I. Rahmawati, and E. Nurharianto, "Membran Blend Kitosan/Poli Vinil Alkohol (PVA): Pengaruh Komposisi material blend, pH, dan Konsentrasi bahan Pengikat Silang", *Jurnal Kimia Riset*, **2**(2), 77, 2017, https://doi.org/10.20473/jkr.v2i2.6195

[49] D. K. Maharani and R. D. Safitri, "Karakterisasi film PVA/kitosan/zeolit tersubtitusi ion Ag+ berpotensi sebagai kemasan aktif", *Unesa Journal of Chemistry*, **11**(1), 46–52, 2022, https://doi.org/10.26740/ujc.v11n1.p46-52

[50] N. Mulchandani, N. Shah, and T. Mehta, "Synthesis of Chitosan-Polyvinyl Alcohol Copolymers for Smart Drug Delivery Application", *Polymers and Polymer Composites*, **25**(3), 241–246, 2017, https://doi.org/10.1177/096739111702500311

[51] G. K. Malik, A. Khuntia, and J. Mitra, "Comparative Effect of Different Plasticizers on Barrier, Mechanical, Optical, and Sorption Properties of Hydroxypropyl Methylcellulose (HPMC)–Based Edible Film," *Journal of*

Biosystem Engineering., **47**(2), 93–105, Jun. 2022, https://doi.org/10.1007/s42853-022-00132-2

[52] S. Poulose, I. Jönkkäri, M. S. Hedenqvist, and J. Kuusipalo, "Bioplastic films with unusually good oxygen barrier properties based on potato fruit-juice", *RSC Advances*, **11**(21), 12543–12548, 2021, https://doi.org/10.1039/D1RA01178B

[53] E. Jamróz, P. Kulawik, and P. Kopel, "The Effect of Nanofillers on the Functional Properties of Biopolymer-Based Films: A Review", *Polymers*, **11**(4), Apr. 2019, https://doi.org/10.3390/polym11040675

[54] G. Cárdenas, J. Díaz, M. F. Meléndrez, and C. Cruzat, "Physicochemical properties of edible films from chitosan composites obtained by microwave heating", *Polymer Bulletin.*, **61**(6), 737–748, 2008, https://doi.org/10.1007/s00289-008-0994-7

[55] A. Jiang *et al.*, "Chitosan Based Biodegradable Composite for Antibacterial Food Packaging Application", *Polymers*, **15**(10), 2023, https://doi.org/10.3390/polym15102235

[56] J. D. Giraldo and B. L. Rivas, "Direct ionization and solubility of chitosan in aqueous solutions with acetic acid", *Polymer Bulletin.*, **78**(3), 1465–1488, 2021, https://doi.org/10.1007/s00289-020-03172-w

[57] M. Marques Gonçalves, D. Florencio Maluf, R. Pontarolo, C. Ketzer Saul, E. Almouazen, and Y. Chevalier, "Negatively charged chitosan nanoparticles prepared by ionotropic gelation for encapsulation of positively charged proteins", *International Journal of Pharmaceutics*, **642**, 123164, 2023, https://doi.org/10.1016/j.ijpharm.2023.123164

[58] F. G. de Carvalho *et al.*, "Synthesis and characterization of TPP/chitosan nanoparticles: Colloidal mechanism of reaction and antifungal effect on *C. albicans* biofilm formation", *Materials Science and Engineering: C*, **104**, 109885, 2019, https://doi.org/10.1016/j.msec.2019.109885

[59] T. Lam, H. Vu, N. Le, Lien, T. Nguyen Ngoc, and P. Dien, "Synthesis and characterization of chitosan nanoparticles used as drug carrier", *Journal of Chemistry*, **44**, 2006.

[60] F. Khoerunnisa *et al.*, "Physicochemical Properties of TPP-Crosslinked Chitosan Nanoparticles as Potential Antibacterial Agents", *Fibers Polymer*, **22**(11), 2954–2964, 2021, https://doi.org/10.1007/s12221-021-0397-z

[61] N. Al-nemrawi, S. Alsharif, and R. Dave, "Preparation of chitosan-tpp nanoparticles: The influence of chitosan polymeric properties and formulation variables", *International Journal of Applied Pharmaceutics*, **10**, 60, 2018, https://doi.org/10.22159/ijap.2018v10i5.26375

[62] K.-I. Jang and H. G. Lee, "Stability of chitosan nanoparticles for L-ascorbic acid during heat treatment in aqueous solution", *Journal of Agricultural and Food Chemistry*, **56**(6),1936–1941, 2008, https://doi.org/10.1021/jf073385e.

[63] M. Akkaya, T. Menlik, A. Sözen, and M. Gürü, "The Effects of Triton X-100 and Tween 80 Surfactants on the Thermal Performance of a Nano-Lubricant: An Experimental Study", *International Journal of Precision Engineering and Manufacturing Green Technology.*, **8**(3), 955–967, May 2021, https://doi.org/10.1007/s40684-020-00280-w

[64] A. Adhyatmika, R. Martien, and H. Ismail, "Preparasi Nanopartikel Senyawa Pentagamavunon-0 Menggunakan Matriks Polimer Kitosan Rantai Sedang dan Pengait Silang Natrium Tripolifosfat Melalui Mekanisme Gelasi Ionik Sebagai Kandidat Obat Antiinflamasi", *Majalah Farmaseutik*, **13**, 65, 2018, https://doi.org/10.22146/farmaseutik.v13i2.40916

[65] S. Tripathy, S. Das, S. P. Chakraborty, S. K. Sahu, P. Pramanik, and S. Roy, "Synthesis, characterization of chitosan-tripolyphosphate conjugated chloroquine nanoparticle and its in vivo anti-malarial efficacy against rodent parasite: a dose and duration dependent approach", *International Journal of Pharmacy*, **434**(1–2), 292–305, 2012, https://doi.org/10.1016/j.ijpharm.2012.05.064

[66] P. F. Vera Garcia *et al.*, "PVA Blends and Nanocomposites, Properties and Applications: A Review", in *Green-Based Nanocomposite Materials and Applications*, F. Avalos Belmontes, F. J. González, and M. Á. López-Manchado, Eds., Cham: Springer International Publishing, 2023, 191–206. https://doi.org/10.1007/978-3-031-18428-4_10

[67] M. Shojaee Kang Sofla, S. Mortazavi, and J. Seyfi, "Preparation and characterization of polyvinyl alcohol/chitosan blends plasticized and compatibilized by glycerol/polyethylene glycol", *Carbohydrate Polymers*, **232**, 115784, 2020, https://doi.org/10.1016/j.carbpol.2019.115784

[68] K. Enoch, R. C. S, and A. A. Somasundaram, "Improved mechanical properties of Chitosan/PVA hydrogel – A detailed Rheological study", *Surfaces and Interfaces*, **41**, 103178, 2023, https://doi.org/10.1016/j.surfin.2023.103178

[69] T. Yang, J. Wu, Y. Yao, K. Wang, Q. Zhang, and Q. Fu, "Towards the toughness-strength balance of poly(vinyl alcohol) films via synergic plasticization", *Polymer*, **301**, 127031, 2024, https://doi.org/10.1016/j.polymer.2024.127031

[70] E. J. Dompeipen, "(Penaeus monodon) WITH INFRARED SPECTROSCOPY," 2017.

[71] E. M. Abdelrazek, I. S. Elashmawi, and S. Labeeb, "Chitosan filler effects on the experimental characterization, spectroscopic investigation and thermal studies of PVA/PVP blend films", *Physica B: Condensed Matter*, **405**(8), pp. 2021–2027, 2010, https://doi.org/10.1016/j.physb.2010.01.095

[72] D. S. More, M. J. Moloto, N. Moloto, and K. P. Matabola, "Silver/Copper Nanoparticle-Modified Polymer Chitosan/PVA Blend Fibers", *International Journal of Polymer Science*, **2021**, 1–12, 2021, https://doi.org/10.1155/2021/6217609

[73] M. H. Buraidah and A. K. Arof, "Characterization of chitosan/PVA blended electrolyte doped with NH4I", *Journal of Non-Crystalline Solids*, **357**(16), 3261–3266, 2011, https://doi.org/10.1016/j.jnoncrysol.2011.05.021

[74] D. Bhumkar and V. Pokharkar, "Studies on effect of pH on cross-linking of Chitosan with sodium tripolyphosphate: A technical note", *AAPS PharmSciTech*, **7**, E50, 2006, https://doi.org/10.1208/pt070250

[75] M. M. AbdElhady, "Preparation and characterization of Chitosan/Zinc Oxide nanoparticles for imparting antimicrobial and UV protection to cotton fabric," *International Journal of Carbohydrate Chemistry*, **2012**, e840591, 2012, https://doi.org/10.1155/2012/840591

[76] R. Priyadarshi, Sauraj, B. Kumar, and Y. S. Negi, "Chitosan film incorporated with citric acid and glycerol as an active packaging material for extension of green chilli shelf life", *Carbohydrate Polymers*, **195**, 329–338, 2018, https://doi.org/10.1016/j.carbpol.2018.04.089

[77] N. P. S. Ayuni, N. W. Yuningrat, and N. W. Citra, "Kajian transpor kreatinin menggunakan membran kitosan-alginat tertaut silang polivinil alkohol (PVA)", *Jurnal Rekayasa Proses*, vol. **12**(2), 56, 2018, https://doi.org/10.22146/jrekpros.38401.

[78] M. Miya, R. Iwamoto, and S. Mima, "FT-IR study of intermolecular interactions in polymer blends", *Journal of Polymer Science: Polymer Physics Edition*, **22**(6), 1149–1151, 1984, https://doi.org/10.1002/pol.1984.180220615

[79] F. Hong *et al.*, "Chitosan-based hydrogels: From preparation to applications, a review", *Food Chemistry: X*, **21**, 101095, 2024, https://doi.org/10.1016/j.fochx.2023.101095

[80] D. Yan, Y. Li, Y. Liu, N. Li, X. Zhang, and C. Yan, "Antimicrobial Properties of Chitosan and Chitosan Derivatives in the Treatment of Enteric Infections," *Molecules*, **26**(23) ,2021, https://doi.org/10.3390/molecules26237136

[81] M. A. Matica, F. L. Aachmann, A. Tøndervik, H. Sletta, and V. Ostafe, "Chitosan as a wound dressing starting material: antimicrobial properties and mode of action", *International Journal of Molecul Science*, **20**(23), 5889, 2019, https://doi.org/10.3390/ijms20235889

[82] P. Sahariah and M. Másson, "Antimicrobial Chitosan and Chitosan Derivatives: A Review of the Structure-Activity Relationship", *Biomacromolecules*, **18**, 2017, https://doi.org/10.1021/acs.biomac.7b01058.

[83] H. Yilmaz Atay, "Antibacterial Activity of Chitosan-Based Systems", in *Functional Chitosan: Drug Delivery and Biomedical Applications*, S. Jana and S. Jana, Eds., Singapore: Springer, 2019, 457–489. https://doi.org/10.1007/978-981-15-0263-7_15

[84] M. Chandrasekaran, K. D. Kim, and S. C. Chun, "Antibacterial activity of chitosan nanoparticles: a review", *Processes*, **8**(9), 2020, https://doi.org/10.3390/pr8091173

[85] S. Suganthi, S. Vignesh, J. Kalyana Sundar, and V. Raj, "Fabrication of PVA polymer

films with improved antibacterial activity by fine-tuning via organic acids for food packaging applications", *Applied Water Science*, **10**(4), 100, 2020, https://doi.org/10.1007/s13201-020-1162-y

[86] E. Tamahkar, "Bacterial cellulose/poly vinyl alcohol based wound dressings with sustained antibiotic delivery", *Chemical Papers*, **75**(8), 3979–3987, 2021, https://doi.org/10.1007/s11696-021-01631-w

[87] D. Pelinescu *et al.*, "Antibacterial Activity of PVA Hydrogels Embedding Oxide Nanostructures Sensitized by Noble Metals and Ruthenium Dye", *Gels*, **9**(8), 2023, https://doi.org/10.3390/gels9080650

[88] R. Goy, D. Britto, and O. Assis, "ArReview of the antimicrobial activity of chitosan", *Polimeros-ciencia E Tecnologia - POLIMEROS*, **19**, 2009, https://doi.org/10.1590/S0104-14282009000300013

[89] C. Verma and M. A. Quraishi, "Chelation capability of chitosan and chitosan derivatives: Recent developments in sustainable corrosion inhibition and metal decontamination applications", *Current Research in Green and Sustainable Chemistry*, **4**, 100184, 2021, https://doi.org/10.1016/j.crgsc.2021.100184

[90] C. Ardean *et al.*, "Factors Influencing the Antibacterial Activity of Chitosan and Chitosan Modified by Functionalization", *International Journal of Molecular Sciences*, **22**(14), 2021, https://doi.org/10.3390/ijms22147449

[91] Y. W. Hasnedi, "Pengembangan Kemasan Cerdas (Smart Packaging) Dengan Sensor Berbahan Dasar Chitosan-Asetat, Polivinil Alkohol, Dan Pewarna Indikator Bromthymol Blue Sebagai Pendeteksi Kebusukan Fillet Ikan Nila", Institut Pertanian Bogor, Bogor, 2009.

[92] A. Pacquit, K. T. Lau, H. McLaughlin, J. Frisby, B. Quilty, and D. Diamond, "Development of a volatile amine sensor for the monitoring of fish spoilage", *Talanta*, **69**(2), 515–520, 2006, https://doi.org/10.1016/j.talanta.2005.10.046

[93] K. I. Oberg, R. Hodyss, and J. L. Beauchamp, "Simple optical sensor for amine vapors based on dyed silica microspheres", *Sensors and Actuators B: Chemical*, **115**(1), 79–85, 2006, https://doi.org/10.1016/j.snb.2005.08.021